Polarization-Controlled Differentiation of Human Neural Stem Cells Using Synergistic Cues from the Patterns of Carbon Nanotube Monolayer Coating

Sung Young Park,[†,‡] Dong Shin Choi,[†] Hye Jun Jin,[‡] Juhun Park,[‡] Kyung-Eun Byun,[‡] Ki-Bum Lee,[§,*] and Seunghun Hong[†,‡,⊥,*]

[†]Interdisciplinary Program in Nano-Science and Technology and [‡]Department of Physics and Astronomy, Seoul National University, Seoul 151-747, Korea, [§]Department of Chemistry and Chemical Biology, Rutgers, The State University of New Jersey, Piscataway, New Jersey 08854, United States, and [⊥]Deparment of Biophysics and Chemical Biology, Seoul National University, Seoul 151-747, Korea

ABSTRACT We report a method for selective growth and structural-polarization-controlled neuronal differentiation of human neural stem cells (hNSCs) into neurons using carbon nanotube network patterns. The CNT patterns provide synergistic cues for the differentiation of hNSCs in physiological solution and an optimal nanotopography at the same time with good biocompatibility. We demonstrated a polarization-controlled neuronal differentiation at the level of individual NSCs. This result should provide a stable and versatile platform for controlling the hNSC growth because CNT patterns are known to be stable in time unlike commonly used organic molecular patterns.

KEYWORDS: neural stem cells · carbon nanotubes · polarization · nanotopography · micropattern

Due to the ability to generate the main phenotypes in the nervous systems, neural stem cells (NSCs) offer great potential in regenerative medicine.[1] For therapeutic applications, such as rebuilding damaged nerves, one should be able to precisely control the direction and structural polarization of individual axonal growth.[2] Previously, attempts have been made to control the structural polarization of cultured neurons by using several key strategies such as molecular cues of diffusible gradient or substrate-bound chemical/extracellular matrix (ECM) protein patterns and topographical cues.[3−12] However, they have several disadvantages. For example, a diffusible gradient is not suitable for the membrane/matrix proteins due to the difficulty of maintaining it over time. In the case of printed protein patterns, the protein molecules may undergo conformational changes during the process of stamping, which often leads to the denaturation and the loss of biological activities.[13] Besides, to create optimal nanotopographical cues which can help cell growth, various micro- or nanofabrication techniques are required, such as electron-beam lithography or chemical/reactive-ion etching.[14] On the other hand, various synthetic nanomaterials such as biocompatible nanofibers and carbon nanomaterials have been recently proposed for novel nanostructured scaffolds.[14−19] However, neuronal polarization control of NSCs, especially at the level of individual axons or dendrites, has not been demonstrated using these nanomaterials.

Herein, we report a method for the structural-polarization-controlled neuronal differentiation of human NSCs (hNSCs) using the patterns of CNT network structures with good biocompatibility. In this strategy, the CNT network patterns provided synergistic cues of selective laminin adsorption and optimal nanotopography, which resulted in selective adhesion and growth of hNSCs on them. CNT network structures were found to induce the enhanced adhesion and growth of hNSCs even better than conventional cell-culture substrates, such as glass. CNT patterns with various geometries were utilized to explore their effect on the outgrowth of hNSC during the growth and differentiation process. As a proof of concept, a structural-polarization-controlled neuronal differentiation using CNT network patterns was demonstrated at the level of individual axons and neurites. Furthermore, we applied our strategy for the controlled hNSC growth on flexible and biocompatible polymer substrates such as polyimide. Since CNT monolayer coatings can be applied to versatile substrates and provide stable microenvironments for hNSC growth control even better than commonly used organic

* Address correspondence to seunghun@snu.ac.kr, kblee@rutgers.edu.

Received for review February 14, 2011 and accepted May 9, 2011.

Published online May 13, 2011
10.1021/nn2006128

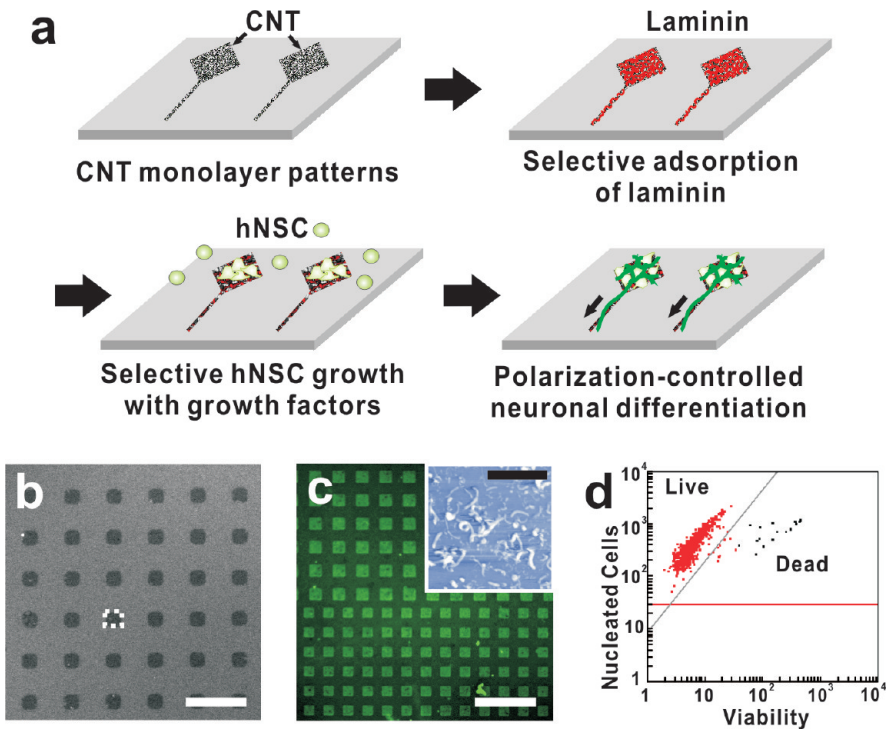

Figure 1. CNT network patterns for selective hNSC growth and polarization. (a) Schematic diagram showing structural-polarization-controlled neuronal differentiation using CNT patterns. CNT monolayer patterns were fabricated on a substrate using a previously reported method,[22] and laminin was absorbed selectively on the CNT-coated regions. This structure induced preferential adhesion of hNSCs, finally achieving structural-polarization-controlled neuronal differentiation. (b) SEM image of CNT patterns (dark spots). Scale bar represents 40 μm. (c) Immunofluorescence image of anti-laminin (green) bound to the laminin which was selectively adsorbed on the CNT patterns. The scale bar represents 200 μm. It confirms the selective adsorption of laminin on the CNT. The inset shows the AFM topography image of the laminin-coated CNT monolayer in phosphate buffered saline (PBS). The scale bar in the inset represents 2 μm. (d) Cell viability assay of hNSCs on CNT patterns for 3 day proliferation. The viability was measured by flow cytometry. The obtained data in the graph clearly indicate that 98% of hNSCs grown on the CNT layer were alive (red).

molecular patterns, our work should provide a simple but efficient way to control the structural polarization of NSCs and may open up various applications in neural engineering and regenerative medicine.

RESULTS AND DISCUSSION

Figure 1a shows a schematic diagram illustrating our basic experimental procedure. CNT patterns were prepared according to previously reported methods.[20,21] Briefly, a self-assembled monolayer (SAM) of methyl-terminated 1-octadecanethiol (ODT) was first patterned on thin Au films on cover glass substrates by microcontact printing, while leaving some bare Au surface regions unaltered (see method in Supporting Information). When the patterned substrate was placed in CNT suspensions (0.05 mg/mL in 1,2-dichlorobenzenne), CNTs were selectively adsorbed onto bare Au regions, forming CNT monolayer patterns. The CNT patterns were then placed in laminin solution (10−20 μg/mL) for 10−30 min so that laminin molecules were selectively adsorbed onto the CNT patterns. Laminin is one of the ECM components that is helpful for hNSC adhesion and growth. After cell seeding, the hNSCs grew preferentially along these laminin-coated CNT patterns in the culture media with growth factors, such as basic fibroblast growth factor (bFGF) and epidermal growth factor (EGF). For hNSCs, the growth factors (bFGF and EGF) are known to enhance hNSC growth and proliferation, while blocking the differentiation process. Afterward, the substrate was placed in culture media without bFGF and EGF for 2 weeks to study the differentiation of hNSCs on laminin-coated CNT patterns.

Figure 1b shows the scanning electron micrograph (SEM) image of the prepared CNT patterns. It shows the well-defined CNT regions (darker square regions) as well as ODT-coated area (lighter region). The high-resolution atomic force microscopy (AFM) image also confirmed the highly selective adsorption of CNTs on bare Au regions (Figure S1a in Supporting Information).

When placed in laminin solution, CNT patterns selectively adsorb laminin molecules from solution. This was verified by immunochemistry (Figure 1c). For this purpose, after the laminin adsorption, the substrate was placed in the fluorescent-labeled anti-laminin solution so that the anti-laminin molecules would bind to the laminin molecules on the substrate. The fluorescence image shows much stronger fluorescence intensity in the CNT regions (brighter green regions in Figure 1c) than on ODT regions, confirming the high-density adsorption

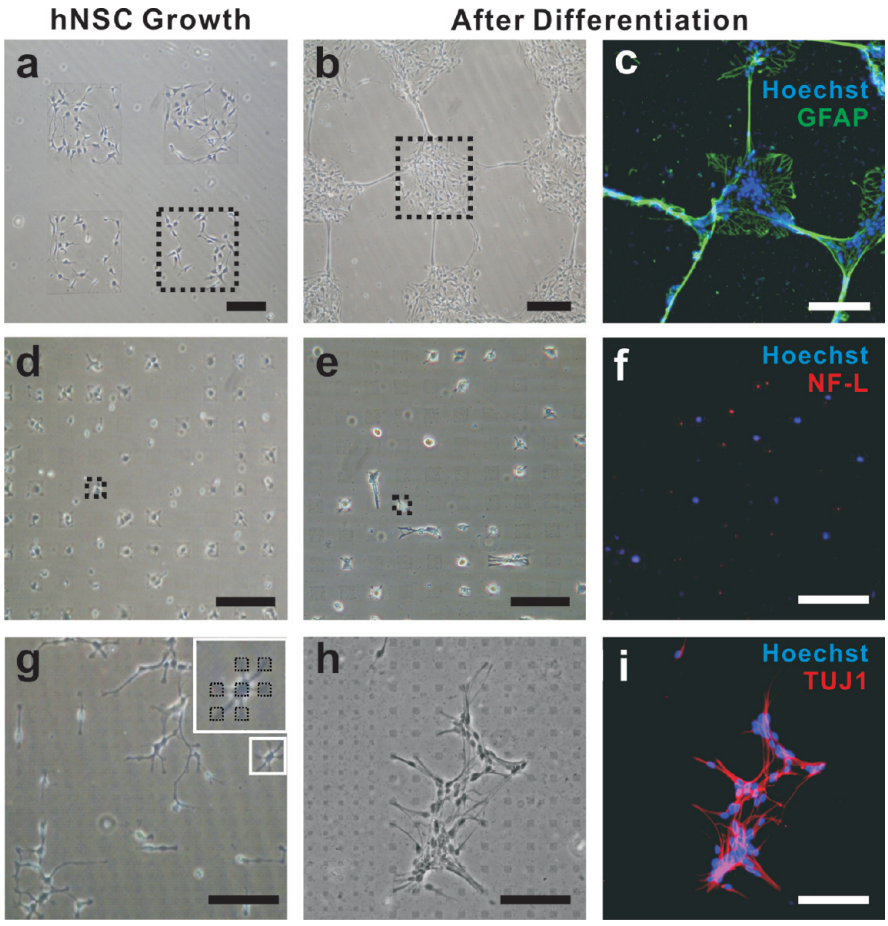

Figure 2. hNSC growth and differentiation depending on the size of CNT patterns. The phase contrast images of hNSCs grown for 1 day (a,d,g) and those of the differentiated cells for 2 weeks (b,e,h), and the immunofluorescence images of the differentiated cells (c,f,i) are shown. The immunofluorescene markers are Hoechst for nuclei, glial fibrillary acidic protein (GFAP) for astroglial cells, and TUJ1 and neurofilament light (NF-L) for neuronal cells. All scale bars represent 200 μm, unless otherwise noted. The dotted black squares (a,b,d,e) indicate some of the CNT-coated regions. (a−c) hNSC growth and differentiation on rather *large* square-shape CNT patterns (300 μm × 300 μm, 200 μm spacing). Note that neural networks were constructed in arbitrary manner after differentiation. The immunofluorescence image (c) shows the differentiated cells positive for the astroglial marker, GFAP (green). (d−f) Restrictive neurite growth of hNSCs in individual CNT square patterns (50 μm × 50 μm, 50 μm spacing). We did not observe any indication of neurite outgrowth of hNSC after the growth and differentiation from the immunostaining image of NF-L (red). (g−i) Outgrowths of hNSCs directed by rather *small* square-shape CNT patterns (5 μm × 5 μm, 5 μm spacing). The inset figure (g) shows that a single hNSC was attached on seven individual CNT square patterns. The immunofluorescence image (i) indicates that the differentiated cells are positive for neuronal cell marker, TUJ1 (red). The scale bar in the phase contrast image (g) represents 100 μm.

of laminin molecules on the CNT patterns. It is also consistent with previous reports regarding the preferential adsorption of protein molecules to CNT sidewalls[22,23] and the resistance of alkyl chains of the ODT SAM to laminin adsorption.[24] The CNT patterns with laminin coating were also investigated *via* an AFM topography image (inset in Figure 1c and Figure S1b in Supporting Information). It exhibited the average roughness of 26 nm, which is in the optimal range of surface roughness (20−50 nm) promoting the adhesion and longevity of primary neurons.[25,26] This result indicates that the nanotopographic cues of CNT network structures as well as laminin molecules adsorbed on the CNT patterns can synergistically induce the selective growth of hNSCs.

The biocompatibility of the CNT network structure as a substrate for hNSC growth was investigated *via* cell viability assay using flow cytometry. For the assay, the adherent hNSCs were detached from the CNT patterns after 3 day growth and 3 day differentiation, respectively. After the 3 day growth period, 98% of the cells were found to be viable (Figure 1d). The assay result of a 3 day differentiation also exhibited nearly 97% cell viability (Figure S2 in Supporting Information). This suggests the good biocompatibility of CNT patterns for hNSC growth and differentiation. Furthermore, we utilized the Western Blot method to confirm the protein expression of hNSCs before and after the differentiation (Figure S3 in Supporting Information). The results show that the hNSCs grown with the growth factors (EGF and bFGF) were positive for neural stem cell markers (nestin and SOX2), which shows that they just proliferated and undifferentiated. Meanwhile, those

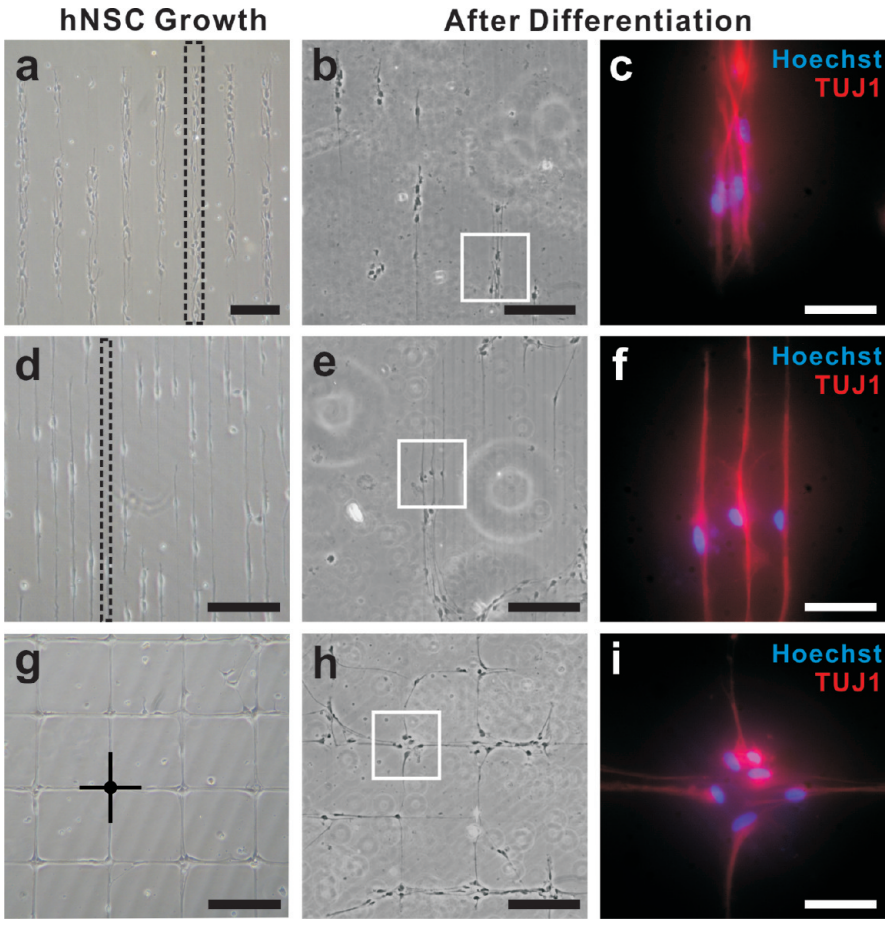

Figure 3. Control of hNSC orientation using line shape CNT patterns. (a–c) hNSC growth on CNT line shape patterns (30 μm width). The hNSCs inside individual 30 μm wide line patterns were observed to grow, extending their neurites in the same direction along the predefined CNT line patterns. (d–f) Individual hNSC growth on each CNT line pattern (5 μm width). The hNSCs were aligned to form a bipolar shape on the CNT line patterns during the growth and differentiation. (g–i) Neural network formed on narrow line shape CNT patterns combined with large square-shape ones. Note that highly oriented hNSC growth was induced by the predefined CNT patterns, and eventually well-organized neural networks were formed after differentiation. (a,d,g) Phase contrast images of hNSC grown for 1 day, and the scale bars in the phase contrast images are 200 μm. (b,e,h) Phase contrast images of the differentiated cell. (c,f,i) Immunofluorescence images of the differentiated cells. The scale bars in the phase contrast images are 50 μm. The dotted black squares indicate some of the CNT-coated regions.

grown without these growth factors were positive for glial fibrillary acidic protein (GFAP) and neuron-specific class III β-tubulin (TUJ1), which indicates that they differentiated.

When the hNSCs were seeded on the laminin-coated CNT patterns in the culture media with the growth factors, they selectively adhered onto the CNT pattern regions and grew along the patterns (Figure 2a,d,g). In this stage, the growth factors blocked the differentiation of hNSCs. When the substrate was placed in the culture media without the growth factors, the hNSCs started to differentiate (Figure 2b,e,h). The differentiation was confirmed by immunocytochemistry (Figure 2c,f,i). Here, we used three different markers to look at cytoskeletal distributions on the CNT patterns after the differentiation: GFAP as an astroglial cell marker (Figure 2c), neurofilament light (NF-L, Figure 2f), and TUJ1 (Figure 2i) as neuronal cell markers. We also performed an experiment to investigate the hNSC growth on CNT networks compared with that on conventional substrates such as coverglass (Figure S5 in Supporting Information). After the hNSC seeding on the laminin-coated CNT patterns that were prepared on coverglass (Figure S5A), we observed that the hNSCs grew selectively in the CNT regions (Figure S5B–D). This result clearly indicates that the CNT network can provide a better extracellular environment for hNSC growth than conventional cell-culture substrates such as coverglass.

Depending on the geometries of CNT patterns, the hNSCs exhibited significantly different outgrowing behaviors during growth and differentiation (Figure 2a–c). When the size of the CNT square patterns was large enough (300 μm $\times$ 300 μm, 200 μm spacing) to hold multiple cells, the hNSCs in the CNT patterns could maintain their cell–cell interactions and proliferated very well (Figure 2a). Eventually, they outgrew over the 200 μm wide ODT SAM regions toward the adjacent

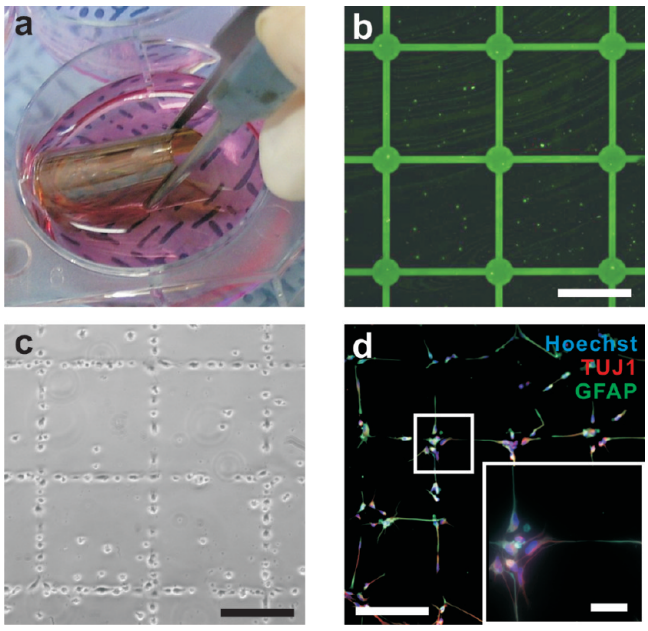

Figure 4. Control of hNSC growth and differentiation on biocompatible and flexible polyimide (PI) substrate. (a) Optical image of a polyimide membrane with CNT patterns, which is flexible and transparent. (b) Immunofluorescence image of antilaminin (green). It confirms that the laminin was selectively adsorbed onto the CNT patterns on PI substrate. Scale bar represents 200 μm. (c) Phase contrast image of selective hNSC adhesion on CNT patterns on PI after cell seeding. Scale bar represents 200 μm. (d) Immunofluorescence image of the differentiated hNSCs on CNT patterns on PI (TUJ1 for neural cells and GFAP for astroglial cells). The inset shows the magnified image of the region marked by the white solid square. Scale bar represents 200 μm, and that of the inset represents 50 μm. It should be noted that the orientation-controlled neural networks were constructed along the CNT patterns on the PI membrane.

CNT square patterns and formed the neural networks, where the cells grown on the distanced CNT square patterns were connected (Figure 2b). The fluorescence image clearly shows that the outgrowing astrocytes (green regions marked as GFAP) were connecting the hNSC population on the distanced patterns after differentiation (Figure 2c).

We then reduced the size of CNT square patterns (50 μm $\times$ 50 μm, 50 μm spacing) such that each square could hold only a single hNSC (Figure 2d–f). In this case, the hNSC outgrowth was extremely restricted during the growth and differentiation process (Figure 2d). Even after we removed the growth factors to induce differentiation, the hNSCs did not exhibit any indication of major outgrowth over the ODT regions (Figure 2e). The fluorescence image of neuronal cytoskeletons (NF-L, red) does not show any outgrowing hNSCs from the patterns (Figure 2f). This result clearly shows that the cell–cell interaction can be controlled by the geometries of CNT patterns, which can be critical for hNSC growth and differentiation.

We also tested hNSC behaviors on CNT square patterns smaller (5 μm $\times$ 5 μm, 5 μm spacing) than individual hNSCs (Figure 2g–i). Here, the hNSCs first adhered and outgrew over several CNT square patterns (Figure 2g). Note that each cell was bound strongly on the small CNT pattern regions and outgrew and extended over the ODT regions. In this case, the spacing of the CNT square patterns should significantly affect the cytoskeletal tensions of the individual hNSCs, which probably should affect the differentiation of stem cells.[27] After the differentiation, we could observe that the neuronal outgrowths extended and bound on the nearby CNT patterns (Figure 2h). The fluorescence image clearly shows the neuronal cytoskeletal marker (TUJ1, green) indicating the connected neural networks bound on the small CNT patterns. Overall, the results in Figure 2 clearly show that the size and spacing of CNT patterns can play a critical role in controlling the hNSC outgrowths during the growth and differentiation process, which can possibly affect cell–cell interactions or cytoskeletal tensions.

Furthermore, line shape CNT patterns can be utilized to control the neuronal orientation with high precision (Figure 3). In the line shape CNT patterns with a line width (30 μm width, 60 μm spacing) that can hold two or three cells, the hNSCs adhered (Figure 3a) along the line pattern. We observed that they differentiated to form neural networks along the inside of the line patterns (Figure 3b). Here, the differentiation was also confirmed by immunocytochemistry with the TUJ1 marker. When the CNT line width was narrowed down to about 5 μm, which can hold only a single hNSC, the hNSCs grew and differentiated into bipolar shapes along the individual CNT line patterns (Figure 3f). Significantly, this result indicates that we can control the orientation of hNSCs with single-cell-level precision.

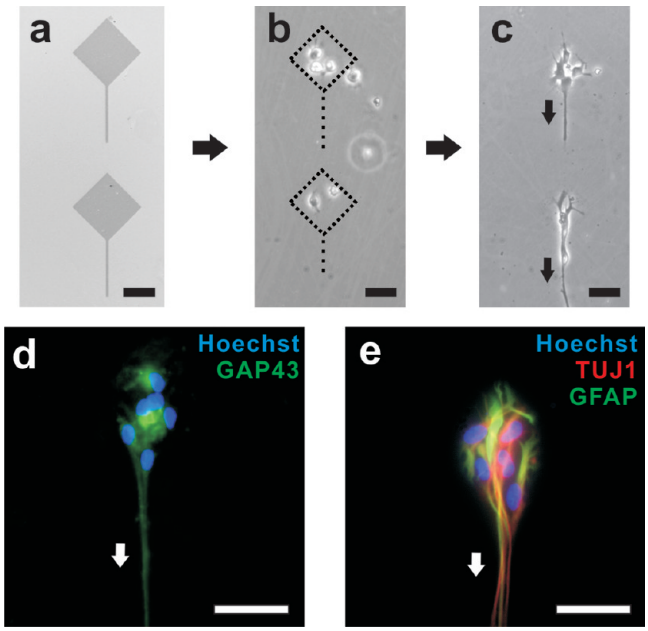

Figure 5. Structural-polarization-controlled neuronal differentiation of individual hNSCs using CNT patterns. (a) SEM image of a CNT pattern with a single narrow strip as shown in dark gray. (b) Phase contrast images of hNSC adhesion on CNT patterns. The dotted square and line (red) represent the CNT patterns. Scale bar represents 50 μm. After cell seeding, the cell bodies of hNSCs were attached within the CNT square region. (c) Phase contrast images of the differentiated cells on the CNT patterns. Note that the growing parts in the hNSCs were observed along the CNT single narrow strip regions during the differentiation. (d) Immunofluorescence images of growth-associated protein 43 (GAP 43, green) and Hoechst (blue, for nucleus). Scale bar represents 50 μm. It should be noted that the GAP 43 (green dots) was distributed along the narrow strip region. (e) Immunofluorescence image of GFAP (green), TUJ1 (red), and Hoechst (blue). Scale bar represents 50 μm. It should be noticed that the differentiated neuronal cells (TUJ1, red) were surrounded by astroglial cells (GFAP, green) on the structural-polarization-controlled CNT pattern, where the neuronal polarization was also directed by the CNT narrow strip region.

When circle-shape patterns are connected with narrow line shape ones, we observed quite an interesting hNSC behavior during the growth and differentiation (Figure 3g–i). After being seeded in the culture media with growth factors, the cell bodies of hNSCs tended to adhere and proliferated on the circle-shape pattern regions (Figure 3g). After withdrawal of the growth factors in the culture media, they started to differentiate and the outgrowing neurites were observed mostly along the narrow line shape CNT pattern regions (Figure 3h). The differentiation was also confirmed *via* immunostaining (Figure 3i). Since the hNSCs first adhered and grew on the circle-shape patterns, their nuclei (blue regions) were mostly located on the circle regions, while the long neurites (red regions) extended along the line shape regions (Figure 3i). This result indicates that the CNT patterns can be utilized to control both of the locations of cell nuclei and the direction of neurite growth, thus allowing us to control the structural polarization of the neuronal differentiation of hNSCs. Furthermore, the synapse formation of the neurons was checked by a neuronal presynaptic vesicle marker, synaptophysin (Figure S6 in Supporting Information). The results clearly show that the neurons differentiated from the hNSCs grown on the CNT patterns can also form the synapses, which are important for a neuron to pass a chemical/electrical signal to another neuron.

For future therapeutic applications, such as regenerative medicine, it would be crucial to apply our strategy to a flexible and biocompatible substrate such as polyimide (PI) (Figure 4), which has been widely utilized for implantable neural devices such as three-dimensional artificial nerve conduits[28] and stimulating electrodes.[29,30] We prepared CNT patterns on thin Au-film-coated PI substrates and performed the experiments of hNSC growth and differentiation on them (Figure 4a). We could achieve high-quality CNT patterns on the Au-coated PI substrates, as shown in the SEM images (Figure S7a in Supporting Information). The immunofluorescence image indicates the highly selective adsorption of laminin onto the CNT patterns on the PI substrate (green regions in Figure 4b). After being seeded on it, the hNSCs adhered selectively onto the CNT pattern regions on PI substrates and proliferated (Figure 4c). Eventually, we achieved the orientation-controlled growth and differentiation of hNSCs along the CNT patterns on the flexible PI substrate (Figure 4d and Figure S7b in Supporting Information).

Finally, the structural-polarization-controlled differentiation of individual hNSCs can be achieved by CNT patterns composed of one square and one line shape (Figure 5a). Here, the width of the line shape region is much smaller than the size of an individual hNSC. After cell seeding, we were able to observe the selective

hNSC adhesion inside the square regions (Figure 5b). Then, the hNSCs on the square region outgrew along the narrow line shape regions during the growth and differentiation stages (Figure 5c). The neuronal differentiation was confirmed by growth associated protein 43 (GAP 43, green in Figure 5d), which is known to be expressed in the growth cone regions of neural cells. We observed that GAP 43 was also highly expressed on the line shape CNT regions, indicating that the neurites outgrew along the line shape regions (Figure 5d and Figure S8 in Supporting Information).

We carried out immunocytochemistry to check the neural lineages of the differentiated cells on these CNT patterns (Figure 5e). Here, GFAP and TUJ1 indicate astroglial and neural cells, respectively. To confirm their lineages, the relative fluorescence intensities of GFAP and TUJ1 from the cell nuclei on the square pattern regions were quantified using a method similar to that reported previously (Figure S9 in Supporting Information).[31] The result shows that 20% of them were TUJ1-positive, whereas another 20% were GFAP-positive. It should be noted that the hNSCs were differentiated with controlled structural polarity on the CNT patterns, while maintaining their capabilities to differentiate into the main phenotypes in the nervous system, such as neuronal or astroglial cells.

CONCLUSION

In summary, we demonstrated a structural-polarization-controlled neuronal differentiation of hNSCs using the patterns of CNT monolayer coating. Due to the synergistic effect of CNT network structures for selective laminin adsorption and optimal nanotopography, we could effectively promote the selective growth of hNSCs on the CNT patterns. The result of the cell viability assay (>97%) suggested the good biocompatibility of CNT patterns for hNSC growth and differentiation. We also confirmed that CNTs could induce the adhesion and growth of hNSCs even better than conventional cell-culture substrates such as bare glass. Importantly, the structural-polarization-controlled neuronal differentiation was demonstrated at the level of an individual axon or neurite. Furthermore, we also applied it to flexible and biocompatible PI substrates, which should significantly expand the possible therapeutic applications of our method. Since CNT monolayer coatings can be applied to versatile substrates including flexible ones and provide a better cell-growth environment than conventional cell-culture substrates such as glass, our strategy should provide many new opportunities in various areas such as neural engineering, stem cell therapy, and regenerative medicine.

EXPERIMENTAL METHODS

Fabrication of CNT Monolayer Patterns. CNT (multiwalled CNT, 98% purified, NanoLab, MA, USA) patterns were fabricated on Au-coated glass substrate according to the methods described previously (Supporting Information).[20,21] To prepare a polymer substrate, polyimide (PI, VTEC Polyimide 1388, Richard Blaine International, Inc., PA, USA) in solution was coated on a cover glass by spin coating at 1000 rpm for 1 min and then cured on a hot plate (Supporting Information). CNT patterns on Au-coated PI were generated by the same method as before.[20,21]

hNSC Culture. Immortalized human NSCs (ReNcell VM, Millipore, Temecula, CA, USA) were purchased and maintained according to the manufacturer's protocol.[32] Differentiation was initiated by removal of growth factors such as basic fibroblast growth factor (bFGF) and epidermal growth factor (EGF) from the culture media, and the cells were allowed to differentiate usually for 2 weeks. For the hNSC culture, the prepared CNT patterns were incubated in laminin solution (20 μg/mL, Sigma, MO, USA) for 30 min. The laminin-coated CNT patterns were washed with PBS several times and subsequently seeded with suspensions of hNSC at a cell density of 10^5/mL. All of the hNSC experiments were carried out between passages 3 and 10.

Cell Viability Assay. The hNSCs were either grown for 3 days or subsequently differentiated for 3 days, and then they were used for cell viability assay. The NSCs were first detached and made into 10^6/mL cell suspensions, of which only a fraction was used for counting cell viability. The cells were incubated with a reagent composed of a mixture of a cell permeant and a noncell permeant dye (ViaCount Reagent, Millipore, Heyward, CA, USA) according to the manufacturer's protocol, and the viability was determined using a single-laser four-color flow cytometry detection system (EasyCyte Plus, Millipore, Heyward, CA, USA) at 500 cells per one flow rate with predefined gating.

Immunocytochemistry. The hNSCs were fixed for 15 min in 4% paraformaldehyde in PBS and permeabilized with 0.1% Triton X-100 in PBS for 15 min, followed by overnight incubation at 4 °C in the following primary antibodies: TUJ1 (1:500; clone SDL.3D10, Sigma, MO, USA), GFAP (1:1000; Dako, Glostrup, Denmark), NF-L (1:200; Millipore, Temecula, CA, USA), GAP 43 (1:200; Millipore, Temecula, CA, USA), and synaptophysin (Millipore, Temecula, CA, USA). Cells were washed with PBS, incubated with either goat anti-mouse FITC (1:200; Sigma, MO, USA) or goat anti-rabbit TRITC (1:500; Sigma, MO, USA), then counterstained with 10 mM Hoechst 33342 (Sigma, MO, USA). The mounted samples were imaged using an inverted fluorescence microscope (Nikon, TE2000, Tokyo, Japan) with an EMCCD monochrome digital camera (DQC-FS, Nikon, Tokyo, Japan). ImageJ software (freely downloadable from National Institutes of Health Web site, http://rsbweb.nih.gov/ij/) was used for subsequent processing of the fluorescence images.

Acknowledgment. We appreciate J.H. Yi and E. Miljan for the fruitful discussion to evaluate NSC culture and differentiation. We also thank A. Solanki, B. Shah, and S. Shah for helpful discussions. This project has been supported by the NRF Grant (No. 2011-0000390), and partial support from the Happy Tech Program (No. 20100020821). S.H. acknowledges the support from the Converging Research Center program (No. 2010K0-01138) and the System 2010 program of the MKE. K.-B.L. acknowledges the NIH Directors' Innovator Award (1DP20D-006462-01) and is also grateful to the NJ commission on Spinal Cord Grant (09-3085-SCR-E-0).

Supporting Information Available: Supplementary methods, additional details on fabrication method, and supplementary figures. This material is available free of charge *via* the Internet at http://pubs.acs.org.

REFERENCES AND NOTES

1. Gage, F. H. Mammalian Neural Stem Cells. *Science* **2000**, *287*, 1433–1438.
2. Reh, T. A. Neural Stem Cells: Form and Function. *Nat. Neurosci.* **2002**, *5*, 392–394.
3. Stenger, D. A.; Hickman, J. J.; Bateman, K. E.; Ravenscroft, M. S.; Ma, W.; Pancrazio, J. J.; Shaffer, K.; Schaffner, A. E.; Cribbs, D. H.; Cotman, C. W. Microlithographic Determination of Axonal/Dendritic Polarity in Cultured Hippocampal Neurons. *J. Neurosci. Methods* **1998**, *82*, 167–173.
4. Lauer, L.; Klein, C.; Offenhausser, A. Spot Compliant Neuronal Networks by Structure Optimized Micro-Contact Printing. *Biomaterials* **2001**, *22*, 1925–1932.
5. von Philipsborn, A. C.; Lang, S.; Loeschinger, J.; Bernard, A.; David, C.; Lehnert, D.; Bonhoeffer, F.; Bastmeyer, M. Growth Cone Navigation in Substrate-Bound Ephrin Gradients. *Development* **2006**, *133*, 2487–2495.
6. Shi, P.; Shen, K.; Kam, L. C. Local Presentation of L1 and N-Cadherin in Multicomponent, Microscale Patterns Differentially Direct Neuron Function *In Vitro*. *Dev. Neurobiol.* **2007**, *67*, 1765–1776.
7. Suter, D. M.; Forscher, P. Substrate-Cytoskeletal Coupling as a Mechanism for the Regulation of Growth Cone Motility and Guidance. *J. Neurobiol.* **2000**, *44*, 97–113.
8. Dertinger, S. K. W.; Jiang, X. Y.; Li, Z. Y.; Murthy, V. N.; Whitesides, G. M. Gradients of Substrate-Bound Laminin Orient Axonal Specification of Neurons. *Proc. Natl. Acad. Sci. U.S.A.* **2002**, *99*, 12542–12547.
9. Mahoney, M. J.; Chen, R. R.; Tan, J.; Saltzman, W. M. The Influence of Microchannels on Neurite Growth and Architecture. *Biomaterials* **2005**, *26*, 771–778.
10. Cai, J.; Peng, X.; Nelson, K. D.; Eberhart, R.; Smith, G. M. Permeable Guidance Channels Containing Microfilament Scaffolds Enhance Axon Growth and Maturation. *J. Biomed. Mater. Res., Part A* **2005**, *75*, 374–386.
11. Dowell-Mesfin, N. M.; Abdul-Karim, M. A.; Turner, A. M.; Schanz, S.; Craighead, H. G.; Roysam, B.; Turner, J. N.; Shain, W. Topographically Modified Surfaces Affect Orientation and Growth of Hippocampal Neurons. *J. Neural Eng.* **2004**, *1*, 78–90.
12. Goldner, J. S.; Bruder, J. M.; Li, G.; Gazzola, D.; Hoffman-Kim, D. Neurite Bridging across Micropatterned Grooves. *Biomaterials* **2006**, *27*, 460–472.
13. von Philipsborn, A. C.; Lang, S.; Bernard, A.; Loeschinger, J.; David, C.; Lehnert, D.; Bastmeyer, M.; Bonhoeffer, F. Microcontact Printing of Axon Guidance Molecules for Generation of Graded Patterns. *Nat. Protoc.* **2006**, *1*, 1322–1328.
14. Seidlits, S. K.; Lee, J. Y.; Schmidt, C. E. Nanostructured Scaffolds for Neural Applications. *Nanomedicine* **2008**, *3*, 183–199.
15. Ferreira, L.; Karp, J. M.; Nobre, L.; Langer, R. New Opportunities: The Use of Nanotechnologies To Manipulate and Track Stem Cells. *Cell Stem Cell* **2008**, *3*, 136–146.
16. Kostarelos, K.; Bianco, A.; Prato, M. Promises, Facts and Challenges for Carbon Nanotubes in Imaging and Therapeutics. *Nat. Nanotechnol.* **2009**, *4*, 627–633.
17. Hu, H.; Ni, Y. C.; Montana, V.; Haddon, R. C.; Parpura, V. Chemically Functionalized Carbon Nanotubes as Substrates for Neuronal Growth. *Nano Lett.* **2004**, *4*, 507–511.
18. Kam, N. W. S.; Jan, E.; Kotov, N. A. Electrical Stimulation of Neural Stem Cells Mediated by Humanized Carbon Nanotube Composite Made with Extracellular Matrix Protein. *Nano Lett.* **2009**, *9*, 273–278.
19. Cellot, G.; Cilia, E.; Cipollone, S.; Rancic, V.; Sucapane, A.; Giordani, S.; Gambazzi, L.; Markram, H.; Grandolfo, M.; Scaini, D.; *et al.* Carbon Nanotubes Might Improve Neuronal Performance by Favouring Electrical Shortcuts. *Nat. Nanotechnol.* **2009**, *4*, 126–133.
20. Rao, S. G.; Huang, L.; Setyawan, W.; Hong, S. Nanotube Electronics: Large-Scale Assembly of Carbon Nanotubes. *Nature* **2003**, *425*, 36–37.
21. Park, S. Y.; Park, S. Y.; Namgung, S.; Kim, B.; Im, J.; Kim, Y.; Sun, K.; Lee, K. B.; Nam, J. M.; Park, Y.; *et al.* Carbon Nanotube Monolayer Patterns for Directed Growth of Mesenchymal Stem Cells. *Adv. Mater.* **2007**, *19*, 2530–2534.
22. Chen, R. J.; Zhang, Y. G.; Wang, D. W.; Dai, H. J. Noncovalent Sidewall Functionalization of Single-Walled Carbon Nanotubes for Protein Immobilization. *J. Am. Chem. Soc.* **2001**, *123*, 3838–3839.
23. Wang, S. Q.; Humphreys, E. S.; Chung, S. Y.; Delduco, D. F.; Lustig, S. R.; Wang, H.; Parker, K. N.; Rizzo, N. W.; Subramoney, S.; Chiang, Y. M.; *et al.* Peptides with Selective Affinity for Carbon Nanotubes. *Nat. Mater.* **2003**, *2*, 196–200.
24. Chang, C. H.; Liao, J. D.; Chen, J. J. J.; Ju, M. S.; Lin, C. C. K. Alkanethiolate Self-Assembled Monolayers as Functional Spacers To Resist Protein Adsorption upon Au-Coated Nerve Microelectrode. *Langmuir* **2004**, *20*, 11656–11663.
25. Fan, Y. W.; Cui, F. Z.; Hou, S. P.; Xu, Q. Y.; Chen, L. N.; Lee, I. S. Culture of Neural Cells on Silicon Wafers with Nano-Scale Surface Topograph. *J. Neurosci. Methods* **2002**, *120*, 17–23.
26. Khan, S. P.; Auner, G. G.; Newaz, G. M. Influence of Nanoscale Surface Roughness on Neural Cell Attachment on Silicon. *Nanomedicine* **2005**, *1*, 125–129.
27. Bray, D. Mechanical Tension Produced by Nerve Cells in Tissue Culture. *J. Cell Sci.* **1979**, *37*, 391–410.
28. Schmidt, C. E.; Leach, J. B. Neural Tissue Engineering: Strategies for Repair and Regeneration. *Annu. Rev. Biomed. Eng.* **2003**, *5*, 293–347.
29. Stieglitz, T.; Beutel, H.; Schuettler, M.; Meyer, J.-U. Micromachined, Polyimide-Based Devices for Flexible Neural Interfaces. *Biomed. Microdevices* **2000**, *2*, 283–294.
30. Lago, N.; Ceballos, D.; Rodriguez, F. J.; Stieglitz, T.; Navarro, X. Long Term Assessment of Axonal Regeneration through Polyimide Regenerative Electrodes To Interface the Peripheral Nerve. *Biomaterials* **2005**, *26*, 2021–2031.
31. Soen, Y.; Mori, A.; Palmer, T. D.; Brown, P. O. Exploring the Regulation of Human Neural Precursor Cell Differentiation Using Arrays of Signaling Microenvironments. *Mol. Syst. Biol.* **2006**, *2*, 37.
32. Donato, R.; Miljan, E. A.; Hines, S. J.; Aouabdi, S.; Pollock, K.; Patel, S.; Edwards, F. A.; Sinden, J. D. Differential Development of Neuronal Physiological Responsiveness in Two Human Neural Stem Cell Lines. *BMC Neurosci.* **2007**, *8*, 36.